Cellulose (2020) 27:1315–1326
https://doi.org/10.1007/s10570-019-02876-1

ORIGINAL RESEARCH

Optical haze regulation of cellulose nanopaper via morphological tailoring and nano-hybridization of cellulose nanoparticles

Li Xinping · Wang Nan · Zhang Xin · Chang Hui · Wang Yaoyu · Zhang Zhao

Received: 9 October 2019 / Accepted: 17 November 2019 / Published online: 23 November 2019

Abstract A series of cellulose nanoparticles (CNPs), including cellulose nanofibrils (CNFs) and cellulose nanocrystals (CNCs-n, n = 1, 2, 3, or 4), was prepared from bleached bamboo pulp. Those CNPs exhibited various morphologies, such as fibrous (CNFs), short rod (CNCs-1), clubbed (CNCs-3), and spherical shapes (CNCs-2 and CNCs-4). The results showed that enzyme pretreatment was feasible for improving crystallinity and size uniformity but also CNP thermal stability. The haze performance of the nanopapers was strongly dependent on CNP morphology. Furthermore, with changes in the hybrid ratio between CNFs and CNCs-2, the transparency of produced nanopapers was maintained at a high level (89–95%). Optical haze was accurately controlled with arbitrary continuous adjustable values in the range of 5–77%. Those cellulose nanopapers with controllable haze offered the potential for applications in light diffusors and flexible optoelectronics.

Electronic supplementary material The online version of this article (https://doi.org/10.1007/s10570-019-02876-1) contains supplementary material, which is available to authorized users.

Li. X · Wang. N · Zhang. X · Zhang. Z (✉)
College of Bioresources Chemical and Materials Engineering, National Demonstration Center for Experimental Light Chemistry Engineering Education, Shaanxi University of Science and Technology, Xi'an 710021, People's Republic of China
e-mail: zhangzhaoqg@sust.edu.cn

Chang. H
College of Mechanical and Electrical Engineering, Shaanxi University of Science and Technology, Xi'an 710021, People's Republic of China

Wang. Y. · Zhang. Z
Northwest University, Xi'an 710069, Shaanxi, People's Republic of China

Graphic abstract

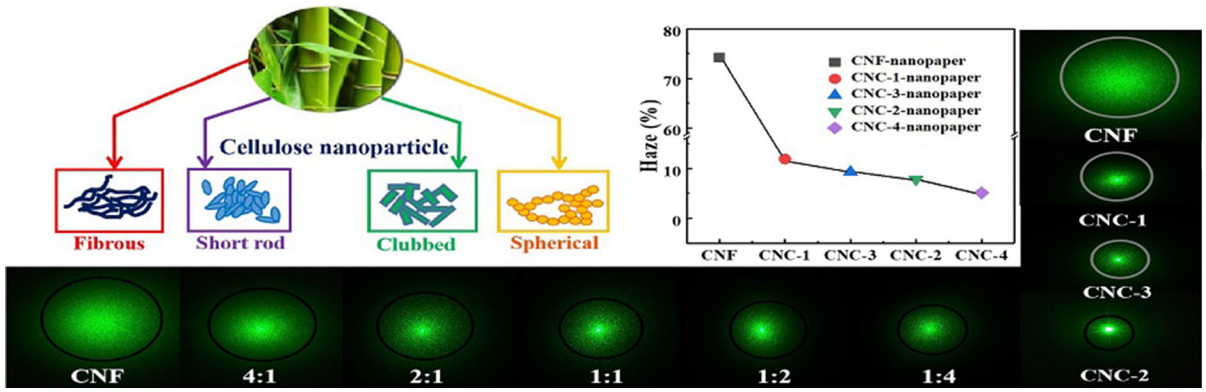

Keywords Bleached bamboo pulp · Enzyme pretreatment · Morphology tailoring · Cellulose nanoparticles · Accurately controlled haze

Introduction

With the progress and development of human society, forest resources are increasingly scarce (Jiang et al. 2010). Bamboo is a grass plant that grows in many parts of the world and is one of the fastest growing plants on the planet. Bamboo fiber is slender and spindle-like, generally 1–2 mm in length, 10–25 μm in width, and with a length–width ratio of 100–200, thus making bamboo fibers fit in the category of long fibers (Trache et al. 2016). The cellulose content of bamboo is between hardwood and general grass fibers but lower than softwood fibers (Wang et al. 2010). Meanwhile, large molecules of bamboo fiber are arranged in an orderly fashion, with a high degree of orientation and high crystallinity. Bamboo, a major nontimber forest product widely distributed in tropical, subtropical, and temperate regions, has been identified as a wood substitute. It is of great scientific and economic value for its potential and high value utilization (Brito et al. 2012).

Cellulose nanoparticles (CNPs) are nano-materials with excellent physical and chemical properties, such as thermal and chemical stability, and biocompatibility. They can be widely used in catalysis, biomedicine and energy storage (Moon et al. 2011). In addition, CNPs with excellent film-formation are usually used to prepare cellulose nanopaper via pressure filtration, evaporation or press-controlled extrusion, giving rise to products with good mechanical properties, processing ability, and low coefficient of thermal expansion (CTE) (Zhang et al. 2018a). Furthermore, nanopapers' low light absorption makes them suitable for application as optical materials (Chen et al. 2018). As a matter of fact, the transparency and hazy properties of CNP nanopapers are closely dependent on their characteristics, such as size, morphology, and crystallinity (Li et al. 2015). Based on Rayleigh's scattering theory ($\delta_{set} \propto D^4$, where δ_{set} is the scattering cross section and D the particle diameter), the haze of cellulose nanopaper closely depends on CNP diameters (Sun et al. 2015; Zhu et al. 2013). Generally, nanopapers prepared from CNCs have high transparency and low haze due to their dense packing structure (Yang et al. 2018). On the contrary, CNFs with a large aspect ratio (length/width) are more likely to become entangled and have air voids after nanopaper formation, giving CNF nanopapers high optical haze. It is difficult to control haze value once the cellulose nanosize has been determined. Recently, CNF composite petroleum-based polymer or post processing with solvent swelling methods has been used to regulate the haze value (Zhu et al. 2013). However, nanohybrids between CNFs and CNCs have been totally ignored. Studies regarding morphological tailoring and nanohybridization of CNPs for optical haze regulation would be advantageous for realizing applications in optoelectronics.

Thus, it was particularly important to explore new means for preparing CNPs with morphological control and tailoring. At present, there are many methods for preparing CNPs, including acid hydrolysis,

mechanical processes, enzymatic hydrolysis, and TEMPO oxidation (Sacui et al. 2014). These methods each have their own merits as well as defects. Among these, acid hydrolysis is a common method used to prepare CNPs from cellulose fibers. The hydrolysis rate with sulfuric acid induces hydrolytic selectivity that is poor for amorphous regions, producing low yield and nonuniform morphology for the resulting CNPs (Cheng et al. 2017). Cellulase is a green biochemical reagent that does not pollute the environment, being a class of enzymes that catalyze cellulose hydrolysis (Tibolla et al. 2014). The low hydrolysis rate of cellulase for cellulose fibers gives rise to CNPs in good to excellent yields, with small nanosize and uniform morphology. It is interesting that regulation of CNP morphology can be achieved via single or multiple hydrolysis strategies. Further studies are needed regarding the relationship between cellulose morphology and haze of resulting nanopapers.

In this paper, a series of CNPs with various morphologies, such as fibrous (CNFs), short rod (CNCs-1), clubbed (CNCs-3), and spherical (CNCs-2 and CNCs-4), were successfully prepared from bleached bamboo pulp. Cellulose nanopapers were prepared using CNFs to achieve an anti-trade-off between transparency (89% at 600 nm) and haze (77%) performance. The transparency of the produced nanopapers was maintained at a high level (89–95%). Meanwhile, optical haze was accurately controlled with arbitrary continuous adjustable values in the range of 5–77% through CNP morphology tailoring and nano-hybridization between CNFs and CNCs-2. The prepared cellulose nanopapers achieved an anti-trade-off between transparency and haze performance that offered the potential for a wide range of applications in light diffusor and flexible optoelectronics (Wang et al. 2019).

Experimental

Materials and instrument

A never-dried bleached bamboo pulp (the moisture content was 70.7%, hemicellulose content was 14.81%, lignin content was 0.64%) was used as cellulose source, which was provided by a Chinese papermaking company. The bleached bamboo pulp was dried under natural conditions for 3 month before use. The enzymatic treatment was carried out in 0.05 M citrate buffer pH 4.8. The citrate buffer was prepared from citric acid monohydrate ($C_6H_8O_7{\cdot}H_2O$), NaOH and distilled water. 210 g of solid citric acid was dissolved in 750 mL of distilled water, the pH of the solution was adjusted to 4.5 with solid NaOH, and the solution was diluted to 1 L. It is diluted 20 times when used and its pH is exactly equal to 4.8. The enzymes was a complex cellulases (endogluconases, exogluconases and B-1,4-gluconases). H_2SO_4, NaOH and $C_6H_8O_7{\cdot}H_2O$ were purchased from Xi'an Kello Instrument Co., Ltd. Scanning electron microscope (SEM) and transmission electron microscopy (TEM) were used to analysis the morphological of CNPs. The obtained thin sheets were coated with gold for 60 s using an ion sputter (Hitachi E-1045, Japan) and then observed with SEM (Hitachi S4800, Japan) at 10 kV. Take a drop of 0.01% of the nanoparticle suspension droplets onto the copper mesh, dry it naturally and observe the morphology with TEM (HITACHI LTD, H-7500). Dynamic light scattering (DLS) experiments were carried out with a Malvern NanoZS instrument at 25 °C and with a detection angle of 173 °C. X-ray diffraction (XRD) patterns were measured using a Bruker–Siemens D8 Advance X-ray diffractometer operated at the Cu Kα radiation (λ = 0.154 nm) with 40 kV and 30 mA in a 2θ range from 5° to 60° at a step size of 0.02°. The chemical state of the element was measured with X-ray photoelectron spectroscopy (XPS, AXIS SUPRA, Shimadzu Company, U.K). XPS spectra of CNF and CNC samples were collected with an Al Kα irradiation (1486.61 eV) at 10 kV and 10 mA current. The thermal stability was characterized using thermogravimetric analysis (TGA) (NETZSCH-Gerätebau GmbH, SDTA 851e model). The samples were heated from 25 to 600 °C at heating rates (20 °C/min) with a nitrogen flow rate of 50 mL/min. The optical haze of the CNFs nanopaper and CNCs-n nanopaper (n = 1, 2, 3 or 4) were obtained using a benchtop colorimetric spectrophotometer (Ci7800, X-Rite, US). The optical transmittance spectra in the UV–Vis region (200–800 nm) were obtained using an ultraviolet–visible spectrophotometer with a 50 W ultraviolet lamp (Cary 5000, Agilent, US).

Preparation of CNF

A 3 g mass of bleached bamboo pulp was added to an Erlenmeyer flask, mixed with pH 4.8 citrate buffer to adjust the slurry concentration to 3 wt%. Then, 5 FPU/g of cellulase solution was added (enzyme dosage refers to enzyme unit weight and dry fiber weight, as FPU/g), then the Erlenmeyer flask was placed in a 50 °C water bath with agitation for 2 h. At reaction's end, the flask was immersed immediately in a boiling water bath for 10 min and then washed three times with distilled water to obtain pretreated fibers. The fibers were diluted with distilled water to a concentration of 2 wt%, the resulting suspension stirred to uniformity, and then passed five times through a high-pressure homogenizer of 80 MPa to obtain CNFs. The obtained CNF samples were dried and the CNF content was determined, indicating that the CNFs yield was 84%.

Preparation of CNC-1

CNC-1 was prepared from bleached bamboo pulp using the acid hydrolysis method. Bleached bamboo fibers (1 g) were added into 60 wt% sulfuric acid adjusts the slurry concentration to 3%, followed by mechanical stirring at 53 °C for 2 h. After reaction, the slurries were poured into a 500 mL beaker with excess deionized water to terminate the reaction. The resultant suspension was centrifuged at 2500 rpm at 25 °C for 15 min, washed with deionized water several times to remove residual acid, and then dispersed under sonication for 5 min to form a stable suspension. Subsequently, a CNC-1 suspension was manufactured by centrifugation at 10,000 rpm at 25 °C for 15 min and repeated several times until the supernatant was light blue. An aliquot of the resulting CNC-1 suspension was dried and the CNC-1 content determined, indicating a yield of 30%.

Preparation of CNC-2

CNC-2 was prepared through a continual process the three-step, including enzyme pretreatment, high-pressure homogenization, and acid hydrolysis (PHA-hydrolysis). The obtained CNFs (1 g) were added into 45 wt% sulfuric acid adjust the slurry concentration to 3%, followed by mechanical stirring at 50 °C for 1 h. After reaction, the slurries were poured into a 500 mL beaker with excess deionized water to terminate the reaction. The resultant suspension was centrifuged at 2500 rpm at 25 °C for 15 min, washed with deionized water several times to remove residual acid, and then dispersed under sonication for 5 min to form a stable suspension. Then, a CNC-2 suspension was manufactured by centrifugation at 10,000 rpm at 25 °C for 15 min and repeated several times until the supernatant was light blue. An aliquot of the resulting CNC-2 suspension was dried and the CNC-2 content determined, indicating a yield of 61%.

Preparation of CNC-3

Bleached bamboo pulp fibers (1 g) were added into an erlenmeyer flask, and mixed with citrate buffer pH = 4.8 adjust the slurry concentration to 3%, and 20 FPU/g cellulase solution was added. Then, the erlenmeyer flask was placed in a constant temperature water bath for stirring treatment at a set temperature 48 °C for 10 h. After the end of the reaction, the cone was immersed in a boiling water bath for 10 min. Further adding distilled water to dilute, the resultant suspension was centrifuged at 2500 rpm for 15 min at 25 °C, washed with deionized water several times to remove residual enzyme, and then dispersed under sonication for 5 min for forming a stable suspension. Subsequently, CNC-3 suspension were manufactured by centrifuged at 10,000 rpm for 15 min at 25 °C and repeat several times until the supernatant is light blue. An aliquot of the resulting CNC-3 suspension was dried and the CNC-3 content determined, indicating a yield of 62%.

Preparation of CNC-4

CNC-4 was prepared through a continual process the three-step, including enzyme pretreatment, high-pressure homogenization, and enzyme hydrolysis (PHE-hydrolysis). The obtained CNF (1 g) were added into an erlenmeyer flask, and mixed with citrate buffer pH = 4.8 adjust the slurry concentration to 3%, and 10 FPU/g cellulase solution was added. The erlenmeyer flask was placed in a constant temperature water bath for stirring treatment at a set temperature 48 °C for 10 h. After the end of the reaction, the cone was immersed in a boiling water bath for 10 min. Further adding distilled water to dilute, the resultant suspension was centrifuged at at 25 °C 2500 rpm for 15 min,

washed with deionized water several times to remove residual enzyme, and then dispersed under sonication for 5 min to form a stable suspension. Then, a CNC-4 suspension was manufactured by centrifugation at 10,000 rpm at 25 °C for 15 min and repeated several times until the supernatant was light blue. An aliquot of the resulting CNC-4 suspension was dried and the CNC-4 content determined, indicating a yield of 76%.

Preparation of CNF nanopaper and CNC-n nanopaper (n = 1, 2, 3 or 4)

Generally, 10 mL of CNCs or CNFs with the concentration of 0.5% was ultrasonically for 5 min, then the CNC suspensions was cast into a disposable culture dish using solution casting method, and then dried in an oven at 40 °C until the film naturally peel off. The CNF suspension was poured onto a microporous membrane coated with 0.22 micron, and vacuum filtration, and then the membrane obtained by suction filtration was dried at room temperature to obtain the CNFs-paper.

Calculation of total haze value

$$Haze = \left(\frac{\tau_4}{\tau_2} - \frac{\tau_3}{\tau_1}\right) \times 100\%$$

τ_4—Scattered light flux of instruments and specimens. τ_3—Instrument scattered light flux. τ_2—Total transmitted light flux through the sample. τ_1—Incident light flux

Calculation of crystallinity index

$$\mathrm{CrI}(\%) = \frac{I_{200} - I_{Am}}{I_{200}} \times 100\%$$

I_{200}—the maximum intensity of (200) lattice diffraction peak. I_{Am}—the intensity scattered by sample amorphous fraction.

Results and discussion

Preparation of CNF, CNC-n, CNF-n nanopaper, and CNC-n nanopaper (n = 1, 2, 3 or 4)

A series of CNPs with different morphologies (fibrous, short rod, clubbed, and spherical) were successfully prepared (Scheme 1). CNCs-1 and CNCs-3 were prepared using sulfuric acid and enzyme hydrolysis from bamboo pulp fibers, respectively. CNFs were prepared by enzyme pretreatment combined with high pressure homogenization, which was further used to prepare CNCs-2 and CNCs-4 via subsequent acid and enzymatic hydrolysis, respectively. The high purity of the bleached bamboo pulp (low content of lignin and hemicellulose), produced CNF yields as high as 84%. Based on related research, CNC-1 yields were generally low, at ~ 30%, when prepared from bamboo fibers by acid hydrolysis. CNCs-2 prepared through three steps (PHA-hydrolysis) showed significantly increased yields, at 61%. CNCs-4, produced through a continual process the three-step PHE-hydrolysis process had the highest yield, at 76%. Enzyme pretreatment destroyed the overall cellulose fiber structure and reduced the energy consumption of CNFs prepared by high-pressure homogenization (Anderson et al. 2014). Such homogenization produced CNFs, which exposed more amorphous regions and allowed acid or enzyme molecules to directly act on amorphous regions, thus avoiding side reactions, such as hydrolysis of crystallization regions, and improving hydrolysis efficiency and increasing product yield.

Morphological analysis

SEM of CNFs showed that dispersed CNFs from bamboo fibers had a fibrous structure (Fig. 1a). The diameters were generally 10–80 nm and the length approximately several microns, which was in agreement with reported results (Mishra et al. 2018). During the freeze-drying process, CNF self-assembled due to strong hydrogen-bonding forces, showing an interwoven network structure (Zhang et al. 2016). In addition, nanofibril lengths were difficult to accurately assess because they were strongly aggregated or engaged, even with homogenization. However, this highly entangled network had a significant influence on the viscoelastic rheological properties of CNF suspensions (M-C Li et al. 2015). CNCs-1 prepared by sulfuric acid hydrolysis of bamboo fibers exhibited short rod shapes with diameters of ~ 90–150 nm and lengths of several hundred nm (Fig. 1b). In sulfuric acid hydrolysis, the amorphous regions with high accessibility were degraded first and then fibers cut or split longitudinally and transversely (Moon et al. 2011). CNFs were interwoven into a network structure with diameters < 100 nm, which were hydrolyzed by sulfuric acid to obtain spherical CNCs-2 (Fig. S1). The diameters of CNCs-2 ranged from 50–100 nm. As

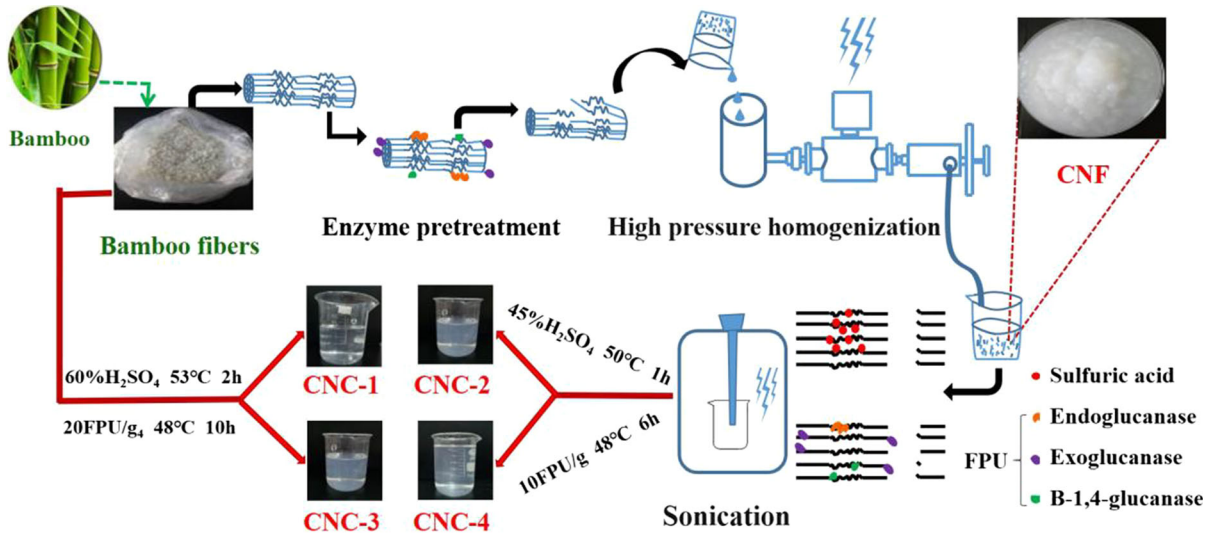

Scheme 1 Preparation of cellulose nanoparticles with different morphologyies

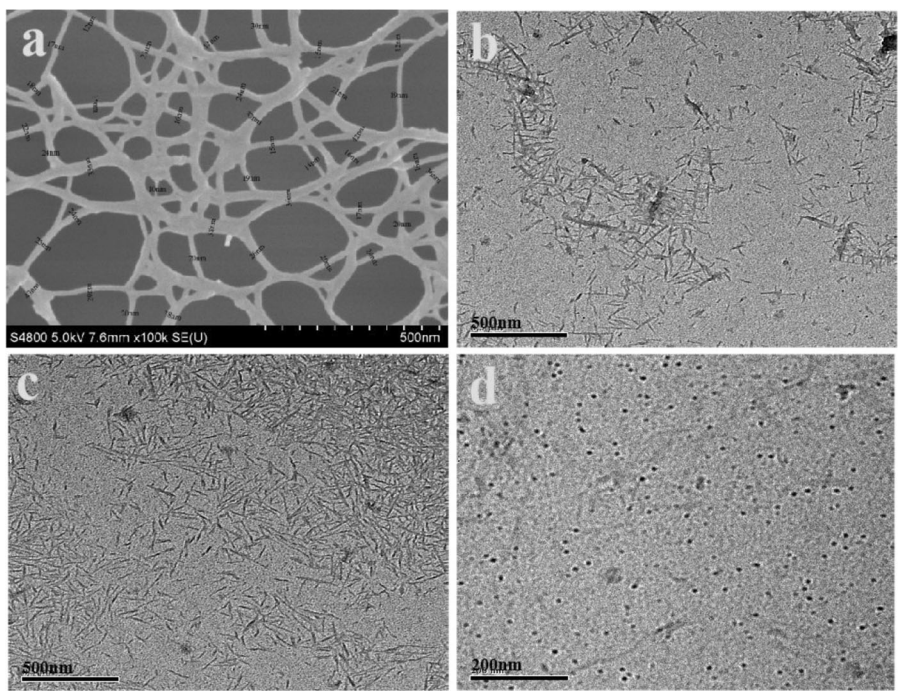

Fig. 1 SEM image of CNF (**a**), TEM images of CNC-1 (**b**), CNC-3 (**c**) and CNC-4 (**d**). Scalar bar 500 nm (**a**–**c**) and 200 nm (**d**)

CNF diameters were in the nanometer scale, most CNF amorphous regions were exposed to more acid molecules. Therefore, under acid hydrolysis, CNF amorphous regions quickly degraded and, at the same time, crystallization zones in the cellulose rapidly hydrolyzed. When the length and diameter were similar, CNCs exhibited a spherical shape.

Bamboo fibers were hydrolyzed by cellulase to produce CNCs-3, which presented clubbed shapes with diameters of ~ 20–70 nm and length of ~

100–400 nm (Fig. 1c). Endonuclease and exonuclease in the complex enzyme acted on fiber surfaces and endonuclease attacked on cellulose amorphous regions, causing the cleavage of glycosidic bonds that shortened the molecular chains and produced polysaccharide chain ends. Exonuclease acting on the ends of cellulose polysaccharide chains, cut fibers into cellobiose units, making the fibers shorter, and producing club-shaped CNCs-3 (Meyabadi et al. 2014; Sacui et al. 2014). However, bamboo fibers hydrolyzed by PHE-hydrolysis produced spherical CNCs-4, with diameters < 50 nm (Fig. 1d). Enzyme pretreatment and high-pressure homogenization caused fibers to produce displacement zones, which are loose regions in the fiber structure into which the enzyme easily penetrates to degrade fibers (Clarke et al. 2011; Li et al. 2012). Therefore, a large number of exposed amorphous and displacement regions in the present preparations allowed cellulase to continuously degrade the material to obtain spherical CNCs-4. The CNF amorphous regions disappeared and the enzyme continued to degrade crystallization zones, further promoting size reduction and PHE-hydrolysis leading to spherical CNCs-4.

Size distribution analysis

The size distribution of CNCs affects its physical properties, such as optical haze and transparency. Nano measurer software was used for analysis of diameter distributions of more than 100 CNCs or CNFs selected randomly from SEM images (Fig. S2 and Table S1). The average diameters of CNCs-1–4 had particle sizes of < 100 nm, which indicated that CNPs were successfully prepared by different methods. For CNCs-1, the reaction procedure involved an acid-induced restructuring process, during the course of which heterogeneous acid hydrolysis involved acid diffusion into cellulose fibers. This resulted in glycosidic bond cleavage within cellulose chains in amorphous domains along the cellulose fibrils, thus leading to hierarchical structure breakdown of fibril bundles into CNCs (Mariano et al. 2014; Ng et al. 2015). CNCs-1 prepared from bamboo fiber by acid-hydrolysis had an average particle diameter of 66 nm and maximum particle diameters of 30 and 129 nm. Due to the high acid hydrolysis rate, smaller-sized CNCs particles were rapidly hydrolyzed, resulting in decreased CNC yields and average size increases. The CNCs-1 size range produced by direct acid-hydrolysis was relatively wide, which was different from PHA-hydrolysis. Enzyme pretreatment and high-pressure homogenization minimized the fiber size and produced displacement zones, while further enhancing amorphous region hydrolysis and endowing CNCs-2 with a narrow size distribution (34–88 nm) and smaller average diameter (46 nm). Enzyme hydrolyzed bamboo fibers obtained CNCs-3 with smaller nanoparticle sizes (26–56 nm). Clearly, CNCs-3 diameters obtained by enzymatic hydrolysis were smaller than CNCs-1 obtained by acid hydrolysis, because the enzyme slowly cut and eroded the fibers. In contrast, acid hydrolysis was intense and rapid and the small-sized CNCs-1 remaining in suspension were degraded in preference to large CNCs-1. Finally, the resulting size was larger than the CNCs-3 sizes obtained by enzymatic hydrolysis. PHE-hydrolysis bamboo fibers were used to prepare CNCs-4 with an 18 nm average diameter and 12-42 nm size range. Therefore, bamboo fibers subjected to enzyme pretreatment, combined with high-pressure homogenization to obtain CNFs and then to enzymatic hydrolysis to obtain CNCs-4, had the highest degree of damage to cellulose fibers as well as the smallest nanoparticle sizes. DLS was also used to determine size distribution (Fig. 2a). Although the particle size distribution did not reflect CNP diameters, it examined overall sizes. The order of particle size was CNCs-1 > CNCs-2 > CNCs-3 > CNCs-4, which was coincident with SEM results. Notably, CNCs-4 exhibited the lowest nano-size and narrowest size distribution, with the largest nano-size and widest distribution observed in CNCs-1. Accordingly, compared with traditional direct acid-hydrolysis, PHE-hydrolysis was very beneficial for preparing uniform and small size CNCs in a high yield.

X-ray diffraction analysis

X-ray diffraction patterns of freeze-dried CNFs and CNCs showed that, as a whole, the main peaks of all samples appeared at 16.5, 22.1, and 34.5, corresponding to cellulose I crystallographic planes. The peak at 16.5 is an overlap of the (1–10) and (110) reflections. The peaks at 22.1 and 34.5 were (200) and (004) reflections, respectively (Fig. 2b; French 2014). These results indicated that both acid and enzymatic hydrolyses did not disrupt all crystal structures in cellulose

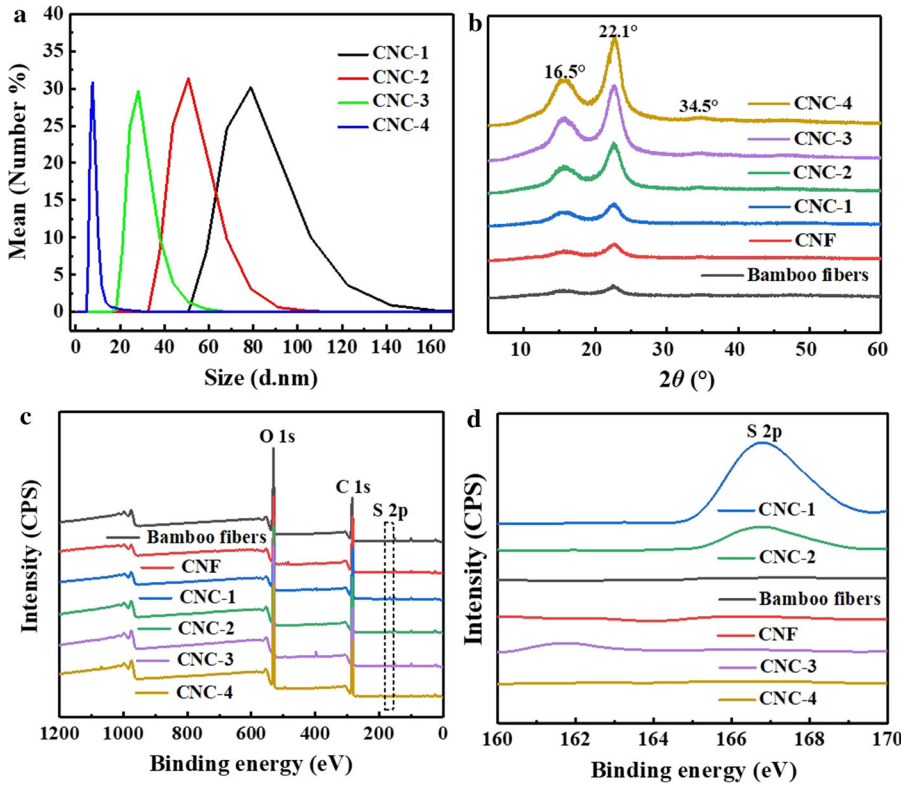

Fig. 2 CNC particle size distribution (**a**); X-ray diffraction patterns of CNC and CNF samples (**b**); XPS survey spectra (**c**) and high-resolution of S 2*p* photoelectron spectra (**d**) of bamboo fiber, CNF, CNC-1, CNC-2, CNC-3 and CNC-4 samples

starting materials and had the polymorphism of cellulose I in CNC samples (Eichhorn 2011). However, the crystallinity index (CrI) was slightly changed under different preparation methods. The crystallinities of CNCs-1 (60.19%) and CNCs-3 (67.06%) were greater than the crystallinity of bamboo fibers (43.89%), while the crystallinities of CNCs-2 (62.38%) and CNC-4 (76.30%) were greater than the CNFs (45.71%), which indicated that acid and enzymatic hydrolyses mainly acted on amorphous regions of bamboo fiber. CNF crystallinity was slightly higher than that of bamboo fiber, indicating that a large number of amorphous regions were exposed after enzymatic pretreatment and homogenization of bamboo fibers. The CNF amorphous regions were more easily eroded or degraded by acid or enzymatic hydrolysis than the bamboo fiber, eventually forming smaller-sized and higher crystallinity CNCs. The segmentation treatment greatly reduced the complete hydrolysis of crystallization zones cellulose during CNC preparation.

X-ray photoelectron spectroscopy

The chemical compositions of bamboo fibers, CNFs, and CNCs were analyzed using XPS. The XPS spectra of bamboo fibers, CNFs, and CNCs showed peaks at 531.0, 284.0, and 167.0 eV for all samples, originating from O-1*s*, C-1*s*, and S-2*p*, respectively (Fig. 2c; Lin & Dufresne 2014). The atomic concentrations of C, O, and S are summarized and listed in Table 1. Hydrogen atoms were not detected by XPS and the S-2*p* peak region in the survey spectra was further confirmed using high-resolution analysis. The S-2*p* peak was absent in the spectra of bamboo fibers, CNFs, CNCs-2, and CNCs-3. However, in the spectra of CNCs-1 and CNCs-2, S-2*p* peaks were observed, with the intensity of these peaks gradually increased with increased acid hydrolysis time, which indicated that more sulfate groups were

Table 1 Elements characteristic of all samples

Sample	Atomic concentration (at.%)		
	C	O	S
Bamboo fibers	63.48	36.52	0
CNF	74.73	25.27	0
CNC-1	70.80	27.58	1.62
CNC-2	64.98	34.72	0.30
CNC-3	66.00	34.00	0
CNC-4	63.30	36.70	0

introduced on CNC surfaces (Fig. 2d). The enzyme pretreatment was benefited to prepare CNCs, which reduced its acid dependence and increased the yield from 30% for CNCs-1 to 61% for CNCs-2.

Thermogravimetric analysis

Thermogravimetric analytical curves (TGA) for bamboo fibers, CNFs, and CNCs-n are shown in (Figs. S3 and S4). The thermal degradation onset temperature (T_0) and maximum decomposition temperature (T_{max}) are listed in Table S2. In the low temperature range (< 120 °C), all samples exhibited a small weight loss due to evaporation of absorbed water and low molecular weight compounds (Dai and Huang 2017). In the high temperature range, the weight loss of all samples differed between samples. Thermal stability is known to be related to several factors, including their dimensions, crystallinities, and extraction conditions. Normally, CNCs with high crystallinity exhibited high thermal stability, but smaller sizes reduced the degradation temperature. For high crystallinity CNCs-1-4, thermal degradation initiated at lower temperatures (160.3, 215.2, 217.8, and 284.4 °C, respectively) than those observed for large size CNFs and bamboo fibers. However, the T_{max} rate of CNCs-1 and CNCs-2 were 233.7 and 271.7 °C, respectively, which were significantly lower than that of bamboo fibers and CNFs. This was explained by the effect in which surface sulfated groups significantly lowered the CNC degradation temperature due to the sulfuric acid elimination, which required less energy in sulfated anhydroglucose units. Compared with the degradation temperature of CNCs-1, CNCs-2 had higher thermal stability, which was attributed to the low content of sulfated groups for CNCs-2. Interestingly, CNCs-3 and CNCs-4 without sulfuric acid units has higher thermal stability than CNCs-1 and CNCs-2, which meant that enzyme pretreatment was helpful for obtaining high thermal stability of CNCs.

Optical properties of nanopapers

During the nanopaper drying process, when water evaporated, smaller nanosized CNPs were densely packed without significant air voids inside the nanopaper, which resulted in high transparency nanopaper (Zhang et al. 2018a). CNC-4 nanopaper exhibited high transmittance (90%) but low haze (5%) in visible light, which was attributed to its smooth surface and densely packed structure (Fig. 3a, b). Nanopaper optical haze decreased from 77 to 5% but was maintained a high transparency (90%). The haze value was 77% for CNF nanopapers and 12, 9, 8, and 5% for CNC-1–4 nanopapers, respectively, which might have resulted from the CNP nanosizes and morphologies. Based on Rayleigh's scattering theory ($\delta_{set} \propto D^4$ where δ_{set} is the scattering cross section and D the CNCs diameter), the haze value of CNCs depended linearly on the D^4. During nanopaper drying, nanosized CNCs were densely packed without significant air voids inside the nanopaper, which was the reason to the nanopaper's high transparency. However, CNF lengths of several or even 100 μm endowed the nanopaper with cross-linking and twine between nanofibril and nanofibril, which induced air voids inside the nanopaper and increased the haze value to 77%. To visualize the light scattering behavior of those transparent cellulose nanopapers, a green laser was applied, which produced a small area spot on the paper. The small radius of the light spot transmitted through the CNC-4 nanopaper indicated that the CNC-4 nanopaper had low haze and produced little light scattering (Fig. 3c, d). CNFs with large nanosize and fibrous morphologies produced a larger and more homogeneously illuminated areas on CNF nanopaper targets, which indicated that the transmitted light was greatly scattered (Zhang et al. 2018b).

Cellulose nanopaper's transparency and optical haze depended on the nano-size and morphology of cellulose particles (Yang et al. 2018, 2019). However, optical haze could not be accurately controlled using arbitrary continuous adjustable values. Enzyme

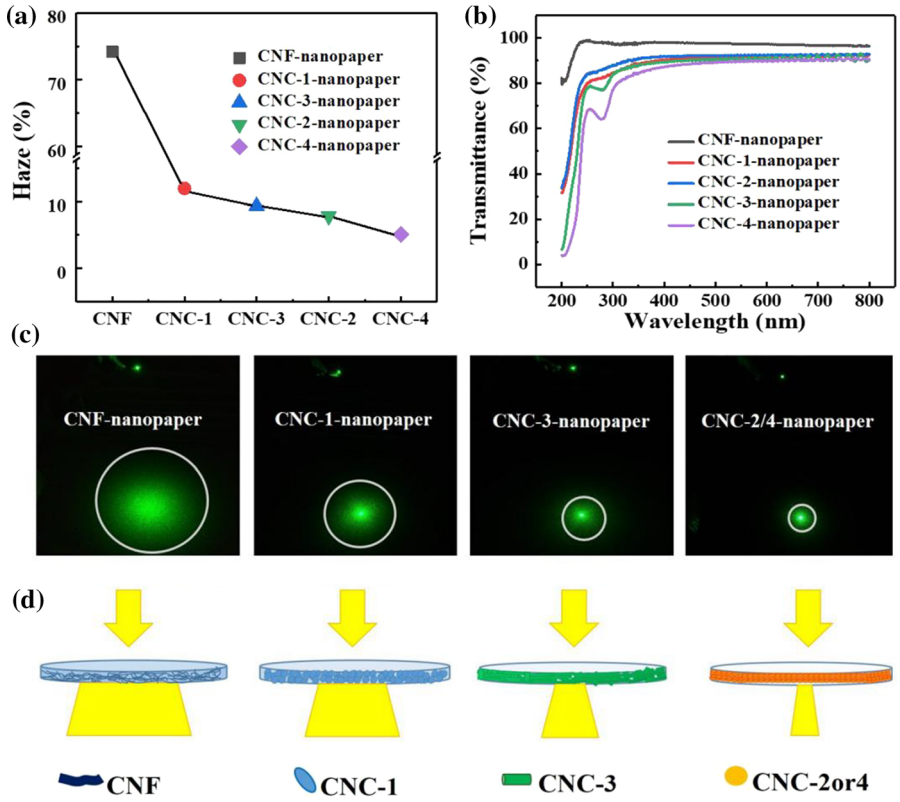

Fig. 3 **a** Haze of nanopapers for different morphologies (fibrous, short rod, clubbed and spherical) cellulose nanoparticle, **b** UV transmission spectra of different nanopapers, **c**, **d** photos of nanopaper for different morphologies cellulose nanoparticle spreading of green laser

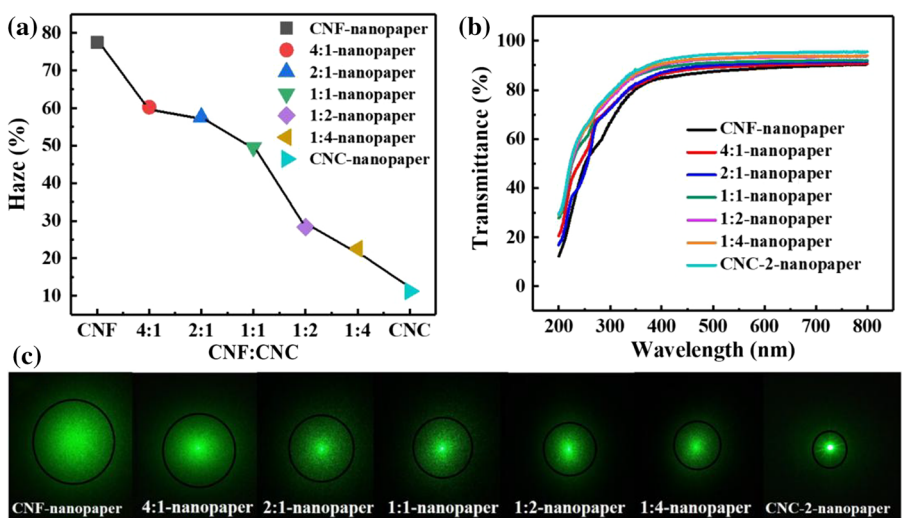

Fig. 4 **a** Haze of nanopapers for CNF and CNC composites in different molar ratio, **b** UV transmission spectra of different nanopapers, **c** photos of CNF and CNC composite nanopaper spreading of green laser

Table 2 Optical properties of different CNF and/or CNC-2 content nanopaper

Sample	Thickness (mm)	Total transmittance (%)	Haze (%)
CNF-nanopaper	0.038 ± 0.002	89	77
4:1-nanopaper	0.030 ± 0.015	90	60
2:1-nanopaper	0.028 ± 0.002	91	58
1:1-nanopaper	0.026 ± 0.001	92	50
1:2-nanopaper	0.024 ± 0.001	93	28
1:4-nanopaper	0.024 ± 0.002	94	23
CNC-1-nanopaper	0.022 ± 0.001	92	12
CNC-3-nanopaper	0.020 ± 0.002	95	9
CNC-2-nanopaper	0.024 ± 0.002	91	8
CNC-4-nanopaper	0.026 ± 0.001	90	5

hydrolysis methods had higher efficiency in preparing CNCs, but the cost was higher than acid hydrolysis. Consideration of the efficiency and cost of preparation of CNPs, CNCs-2 were produced in enormous quantities via PHA-hydrolysis for further research. In addition, CNF and CNC-2 nanopapers exhibited the highest and lower optical haze, respectively (Fig. 4a). It was interesting to obtain arbitrary continuous adjustable haze values using a simple method of compositing CNFs and CNCs-2. Many air voids and layer gaps inside CNF nanopapers induced high optical haze. The smaller nanosize CNC-2 composite with CNFs filled in those air voids and layer gaps, achieving a form of light scattering regulation. The air voids and layer gaps inside the nanopaper resulted in a thicker nanopaper (0.038 mm). In a certain area and quality of nanopaper, the thickness gradually decreased with increased CNF content, which further demonstrated CNC-2 filling of CNF pack voids or layer–layer gaps (Table 2). There was a positive correlation between the optical haze value and CNF content in CNFs/CNCs composite nanopapers. Optical haze value was enhanced from 23 to 60% with gradually increased CNF/CNC-2 molar ratios from 1/4 to 4/1. It was important to control optical haze and here it was adjusted over a wide range from 77 to 11% while nanopaper transparency was sustained in at a high value (89%, Fig. 4b). As expected, these composite nanopapers exhibited a variety of light scattering and diffusion abilities (Fig. 4c). Tailoring CNP morphology, which achieved transparent and hazy regulation that offered the potential for a wide range of applications in light diffusor and flexible optoelectronics (Zhang et al. 2019).

Conclusions

A series of CNPs with various morphologies (fibrous, short rod, clubbed, and spherical) were successfully prepared. The results showed that CNPs were well crystallized with a narrow size distribution. Cellulose nanopapers were prepared using CNFs to achieve an anti-trade-off between transparency (89% at 600 nm) and haze (77%) performance. With changes in CNP morphology and production of composite CNFs and CNCs, the transparencies of the produced nanopapers were maintained at a high level and the optical haze accurately controlled with arbitrary continuous adjustable values. The CNPs developed here achieved an anti-trade-off between transparency and haze performance, which offered the potential for a wide range of applications in light diffusor and flexible optoelectronics.

Acknowledgments This work was supported by National Natural Science Foundation of China (No. 21703131, 31370578), Doctoral Scientific Research Foundation of Shaanxi University of Science and Technology (No. 2016BJ-40), State Key Laboratory of Pulp and Paper Engineering (No. 201821), Special Research Fund by Shaanxi Provincial Department of Education (No. 18JK0122), Chinese Postdoctoral Science Foundation (No. 2018M643707), and Natural Science Basic Research Plan in Shaanxi Province of China (No. 2019JQ-516).

References

Anderson SR, Esposito D, Gillette W, Zhu J, Baxa U, Mcneil SE (2014) Enzymatic preparation of nanocrystalline and microcrystalline cellulose. Tappi J 13:35–42

Brito BL, Pereira FV, Putaux JL, Jean B (2012) Preparation, morphology and structure of cellulose nanocrystals from bamboo fibers. Cellulose 19:1527–1536

Chen X, Wei W, Fan N, Su Y, Ai Y, Qiu QF, Su CY (2018) Visualization of anisotropic and stepwise piezofluorochromism in an MOF single crystal. Chem 11:2658–2669

Cheng M, Qin Z, Chen Y, Hu S, Ren Z, Zhu M (2017) Efficient extraction of cellulose nanocrystals through hydrochloric acid hydrolysis catalyzed by inorganic chlorides under hydrothermal conditions. ACS Sustain Chem Eng 5:4656–4664

Clarke K, Li X, Li K (2011) The mechanism of fiber cutting during enzymatic hydrolysis of wood biomass. Biomass Bioenergy 35:3943–3950

Dai H, Huang H (2017) Synthesis, characterization and properties of pineapple peel cellulose-*g*-acrylic acid hydrogel loaded with kaolin and sepia ink. Cellulose 24:69–84

Eichhorn SJ (2011) Cellulose nanowhiskers: promising materials for advanced applications. Soft Matter 7:303–315

French AD (2014) Idealized powder diffraction patterns for cellulose polymorphs. Cellulose 21:885–896

Jiang L, Chen F, Qian J, Huang J, Wolcott M, Liu L, Zhang J (2010) Reinforcing and toughening effects of bamboo pulp fiber on poly(3-hydroxybutyrate-co-3-hydroxyvalerate) fiber composites. Ind Eng Chem Res 49:572–577

Li X, Clarke K, Li K, Fougere JD, Chen A (2012) Accelerated hydrolysis rate due to fiber cutting throughout enzymatic cellulose hydrolysis. J Bioprocess Eng Biorefinery 1:77–85

Li MC, Wu Q, Song K, Lee S, Qing Y, Wu Y (2015) Cellulose nanoparticles: structure-morphology-rheology relationships. ACS Sustain Chem Eng 3:821–832

Lin N, Dufresne A (2014) Surface chemistry, morphological analysis and properties of cellulose nanocrystals with gradiented sulfation degrees. Nanoscale 6:5384–5393

Mariano M, El Kissi N, Dufresne A (2014) Cellulose nanocrystals and related nanocomposites: Review of some properties and challenges. J Polym Sci Part B: Polym Phys 52:791–806

Meyabadi TF, Dadashian F, Sadeghi GM, Asl HZ (2014) Spherical cellulose nanoparticles preparation from waste cotton using a green method. Powder Technol 261:232–240

Mishra RK, Sabu A, Tiwari SK (2018) Materials chemistry and the futurist eco-friendly applications of nanocellulose: status and prospect. J Saudi Chem Soc 22:949–978

Moon RJ, Martini A, Nairn J, Simonsen J, Youngblood J (2011) Cellulose nanomaterials review: structure, properties and nanocomposites. Chem Soc Rev 40:3941–3994

Ng H-M, Sin LT, Tee T-T, Bee S-T, Hui D, Low C-Y, Rahmat AR (2015) Extraction of cellulose nanocrystals from plant sources for application as reinforcing agent in polymers. Compos Part B Eng 75:176–200

Sacui IA, Nieuwendaal RC, Burnett DJ, Stranick SJ, Jorfi M, Weder C (2014) Comparison of the properties of cellulose nanocrystals and cellulose nanofibrils isolated from bacteria, tunicate, and wood processed using acid, enzymatic, mechanical, and oxidative methods. ACS Appl Mater Interfaces 6:6127–6138

Sun X, Wu Q, Ren S, Lei TC (2015) Comparison of highly transparent all-cellulose nanopaper prepared using sulfuric acid and TEMPO-mediated oxidation methods. Cellulose 22:1123–1133

Tibolla H, Pelissari FM, Menegalli FC (2014) Cellulose nanofibers produced from banana peel by chemical and enzymatic treatment. LWT Food Sci Technol 59:1311–1318

Trache D, Hussin MH, Chuin CH, Sabar S, Fazita MN, Taiwo OA (2016) Microcrystalline cellulose: Isolation, characterization and bio-composites application: a review. Int J Biol Macromol 93:789–804

Wang Y, Wang G, Cheng H, Tian G, Liu Z, Xiao Qun F, Gao X (2010) Structures of bamboo fiber for textiles. Text Res J 80:334–343

Wang Z, Zhu CY, Mo JT, Fu PY, Zhao YW, Yin SY, Su CY (2019) White light emission from dual-way photon energy conversion in a dye-encapsulated metal-organic framework. Angew Chem 29:9752–9757

Yang W, Jiao L, Liu W, Deng Y, Dai H (2018) Morphology control for tunable optical properties of cellulose nanofibrils films. Cellulose 25:5909–5918

Yang W, Jiao L, Liu W, Dai H (2019) Manufacture of highly transparent and hazy cellulose nanofibril films via coating TEMPO-oxidized wood fibers. Nanomaterials 9:107

Zhang T, Zheng Y, Cosgrove DJ (2016) Spatial organization of cellulose microfibrils and matrix polysaccharides in primary plant cell walls as imaged by multichannel atomic force microscopy. Plant J 85:179–192

Zhang Z, Chang H, Xue B, Zhang S, Li X, Wong WK, Li K, Zhu X (2018a) Near-infrared and visible dual emissive transparent nanopaper based on Yb(III)–carbon quantum dots grafted oxidized nanofibrillated cellulose for anti-counterfeiting applications. Cellulose 25:377–389

Zhang Z, Zhang M, Li X, Li K, Lü X, Wang Y, Zhu X (2018b) Irreversible solvatochromic Zn-nanopaper based on Zn(II) terpyridine assembly and oxidized nanofibrillated cellulose. ACS Sustain Chem Eng 6:11614–11623

Zhang Z, Song F, Zhang M, Chang H, Zhang X, Li X, Zhu X, Lü X, Wang Y, Li K (2019) Cellulose nanopaper with controllable optical haze and high efficiency ultraviolet blocking for flexible optoelectronics. Cellulose 26:2201–2208

Zhu H, Parvinian S, Preston C, Vaaland O, Ruan Z, Hu LN (2013) Transparent nanopaper with tailored optical properties. Nanoscale 5:3787–3792